四川大学学报（医学版） 2024，55（6）：1396－1402
J Sichuan Univ（Med Sci）

在线全文

可移动脑磁图阵列可有效采集平原健康人群初级听觉诱发的响应信号*

袁 媛[1]，陈正举[2]，孙 伟[2]，付诗琴[2]，金 琳[3]，盛经纬[4]，孟秋建[3]，武江芬[4]，陈 蕾[5]，幸浩洋[2,6△]

1. 四川大学华西医院 健康管理中心（成都 610041）；2. 四川大学华西医院 放射科 放射影像研究所（成都 610041）；
3. 北京昆迈医疗科技有限公司（北京 100195）；4. 北京大学前沿交叉学科研究院 磁共振成像研究中心（北京 100871）；
5. 四川大学华西医院 神经内科（成都 610041）；6. 四川大学物理学院（成都 610064）

【摘要】 目的 探讨可移动(指探测器到颞叶头皮的距离可以移动)阵列光泵磁力仪脑磁图(optically pumped magnetometers-magnetoencephalography, OPM-MEG)是否可以有效采集平原健康受试者听觉诱发的响应信号，为后续在长期高原居住人群中探讨脑功能变化提供有益的技术参考。**方法** 本研究共招募了40名平原(海拔470 m)健康受试者，通过调整两侧颞叶探测器与头皮的距离，比较不同距离下(0 mm、5 mm、10 mm、15 mm)的颞叶听觉响应信号，分析每个被试在不同距离下的M100峰值信号强度、噪声、信噪比和潜伏期，以及对应的听觉溯源定位图。通过单因素检验，比较在不同距离下，探测器响应信号的差异。**结果** 随着探测器与头皮距离的增加，噪声、信号、信噪比逐渐衰弱(P<0.001)；噪声和信号呈线性衰减趋势，但信噪比在5 mm时值最大，并未呈现出线性衰减的趋势；潜伏期不受距离影响(P=0.72)；溯源定位结果基本一致。**结论** 探测器和头皮的距离在5 mm时，信噪比值最高，能够达到高灵敏度和高信号强度。即使探测距离达到15 mm，OPM-MEG信噪比依然高于16 dB，能够满足临床的信号采集需求；进一步，溯源定位结果也基本一致，距离变化并不会影响溯源结果的可用性，证实了该设备的信号采集有效性。

【关键词】 光泵磁力仪 脑磁图 距离 信号 信噪比

Movable Array of Magnetoencephalography With Optically Pumped Magnetometers Effectively Captures Primary Auditory-Evoked Response Signals in Healthy Populations at Low Altitudes

YUAN Yuan[1], *CHEN Zhengju*[2], *SUN Wei*[2], *FU Shiqin*[2], *JIN Lin*[3], *SHENG Jingwei*[4], *MENG Qiujian*[3], *WU Jiangfen*[4], *CHEN Lei*[5], *XING Haoyang*[2,6△]. 1. *Health Management Center, West China Hospital, Sichuan University*, Chengdu 610041, China; 2. *Institute of Radiology and Medical Imaging, Department of Radiology, West China Hospital, Sichuan University*, Chengdu 610041, China; 3. *Beijing Quanmag Healthcare*, Beijing 100195, China; 4. *Center for MRI Research, Academy for Advanced Interdisciplinary Studies, Peking University*, Beijing 100871, China; 5. *Department of Neurology, West China Hospital, Sichuan University*, Chengdu 610041, China; 6. *College of Physics, Sichuan University*, Chengdu 610064, China

△ Corresponding author, E-mail: xhy@scu.edu.cn

【Abstract】 Objective To investigate the effectiveness of a movable (with the distance between the temporal scalp and the detector being adjustable) array of optically pumped magnetometers for magnetoencephalography (OPM-MEG) in capturing auditory evoked response signals in healthy subjects living at low altitudes, and to provide a useful technical reference for subsequent exploration of the changes in brain functions in populations living at high altitudes on a long-term basis. **Methods** Forty healthy subjects living at a low altitude (470 m above sea level) were recruited. The distance between the scalp and the bilateral temporal lobe detector was adjusted, and the subjects' auditory responses in the temporal lobes were recorded at the distances of 0 mm, 5 mm, 10 mm, and 15 mm. For the different distances, the M100 peak signal strength, noise, signal-to-noise ratio (SNR), and latency were analyzed along with the corresponding auditory source localization maps. A single-factor analysis of variance was conducted to compare the differences in response signals at varying distances. **Results** As the distance between the scalp and the detector increased, the noise, the signal, and the SNR gradually weakened (P<0.001). The noise and signal showed a tendency of linear decline. On the other hand, the SNR reached its maximum at 5 mm and did not show a tendency of linear decline. Latency was not affected by the distance (P=0.72). The results of the auditory stimulus source reconstruction were generally consistent. **Conclusion** When the distance between the detector and the scalp is 5 mm, the SNR value is the highest, resulting in high sensitivity and high signal strength. On the other hand, even when the distance between the detector and the scalp reaches 15 mm, the SNR of the OPM-MEG is still higher than 16 dB, which meets the clinical signal acquisition

* 四川大学华西医院横向合作项目(No. HX-H2304118)资助

△ 通信作者，E-mail: xhy@scu.edu.cn

出版日期：2024-11-20

requirements. Furthermore, the auditory stimulus source reconstruction results were generally consistent. Changing the scalp-to-detector distance does not affect the applicability of the source localization results, validating the device's effectiveness in signal acquisition.

【Key words】 Optically pumped magnetometers　Magnetoencephalography　Distance　Signals　Signal-to-noise ratio

高原缺氧环境对脑功能的影响及其预防机制是当前的研究热点[1-3]。脑磁图(magnetoencephalography, MEG)凭借亚毫秒级时间分辨率和毫米级空间分辨率[4], 为研究高原缺氧环境对脑功能的影响提供了有力的技术手段[5]。目前MEG技术主要分为超导量子干涉器件(superconducting quantum interference devices, SQUID)[6]和光泵磁力仪(optically pumped magnetometers, OPM)。与成本高且需固定在杜瓦瓶中的SQUID-MEG[7-8]不同, OPM-MEG无需冷却隔热, 探测器可以更靠近头皮的位置, 甚至直接接触皮肤[9-10], 从而在增强信号强度[11-13]的同时大幅降低了成本。

作为一种新兴技术, OPM-MEG的研究与应用尚处于起步阶段。理论上, 为了信号强度最大化, 探测器阵列应尽量靠近头皮。然而, 在实际应用中, 探测器到头皮的距离难以完全标准化。为进一步探究探测器到头皮距离对信号质量的影响, 本研究通过可移动OPM探测器阵列, 系统分析不同距离下平原健康人群听觉诱发响应信号的变化情况。本研究旨在验证OPM-MEG信号采集的有效性, 为后续在长期高原居住人群中探讨脑功能变化提供有益的技术参考。

1　资料与方法

1.1　主要仪器

本研究使用的是国内自主研制的科研型OPM-MEG(北京昆迈医疗科技有限公司), 见图1A。该机型适用于不同头型的脑磁信号采集, 可针对性地进行探测器的距离调整。OPM-MEG设备主要由屏蔽筒、采集阵列、采集床和控制系统组成。

1.2　研究对象

本研究为早期探索性临床研究, 于2023年9月26日–2023年10月20日在四川大学华西医院放射科放射影像研究所招募了40名健康受试者(海拔470 m), 男性和女性各20名。纳入标准: ①身体健康且听力、视力(矫正视力)正常; ②年龄: 20 ~ 35岁; ③无癫痫、精神系统疾病病史, 无严重系统性疾病病史。排除标准: ①体内有金属植入物; ②有幽闭恐惧症; ③头部磁共振成像(magnetic resonance imaging, MRI)检查显示结构性病变。本研究经四川大学华西医院伦理委员会审核批准, 批准号: 2023年审(1692)号。所有受试者均给予书面知情同意。

1.3　研究方法

受试者采集4组听觉刺激信号, 每组约4 min, 各组信号对应探测器和头皮的距离分别是: 0 mm、5 mm、10 mm、15 mm(以0 mm为测试起点)。信号采集过程中, 受试者仰卧, 睁眼保持清醒状态, 同时头部及身体尽量不要活动, 以减少因轻微活动造成的信号误差, 见图1B。两侧颞叶的OPM探测器安装在3D打印的头盔中, 两侧各有7个探测器以贴合覆盖颞叶, 可通过旋钮来控制OPM探测器与头皮的距离, 见图1C。

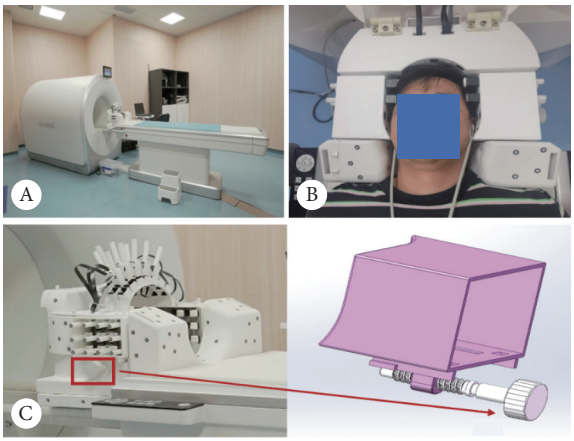

图 1　OPM-MEG设备

Fig 1　The OPM-MEG device

A, The OPM-MEG device of the Clinical Magnetic Resonance Research Center, Department of Radiology, West China Hospital, Sichuan University. B, The subject was lying on the acquisition bed in a supine position. The detector was positioned close to the scalp and covered the temporal lobe in the initial state. C, The modulation knobs of the detector were located on the left and right sides of the helmet to adjust the distance between the detector and the scalp.

1.4　信号采集

听觉刺激使用基于MATLAB的Psychtoolbox工具箱实现。在安静的环境下, 受试者佩戴空气耳机听取声音刺激, 以1 kHz纯音调作为标准刺激, 刺激时长约50 ms, 刺激间隔为0.8 ~ 1.1 s随机, 标准刺激重复200次。为使受试者集中注意力, 在标准刺激中会混入500 Hz纯音调作为异常刺激(outlier), 数量为标准刺激数量的5% ~ 8%, 要求受试者在听到outlier后按键。任务期间同步采集OPM-MEG信号, 采样率为1 kHz。数据采集前, 使用光学扫描仪(EXScanHX, 先临三维科技股份有限公司)进行光学扫描, 记录受试者面部、头盔和探测器位置信息, 获得受试者面部点云文件以及头盔框架点文件, 用于后续

MEG和MRI配准。

3D-T1WI数据采用西门子3T扫描仪(Trio Tim, Erlangen, Germany)获得,使用32通道相控阵头线圈。在扫描过程中,耳塞被用来减少噪音,耳垫被用来减少头部运动。3D T1图像的扫描参数如下:磁化制备快速梯度回波序列;重复时间/回波时间=1900 ms/2.2 ms;翻转角度=9°;切片厚度=1 mm;矩阵=256×256;视场=256 mm×256 mm。

1.5 数据分析

MEG大部分处理及分析基于MNE-Python工具包完成。预处理包括50 Hz的陷波和4 ~ 40 Hz带通滤波。以非重叠的800 ms(刺激开始前200 ms作为基线)的时间窗对数据进行分段。随后对坏通道进行插值和剔除伪迹过大的试次,对剩余的试次进行叠加平均和26 ms的延迟校正,确定信噪比和M100的潜伏期。具体数据处理流程见图2。

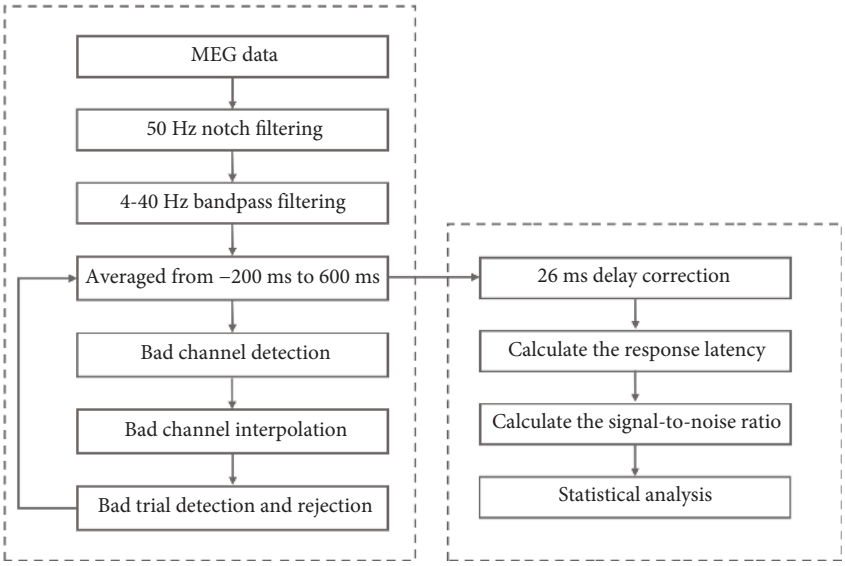

图 2 MEG数据的分析流程

Fig 2 Flow chart of MEG data analysis

使用四分位距(interquartile range, IQR)异常值检测方法进行坏通道与坏试次检测,将上下四分位外1.5倍IQR作为异常值阈值。对基线(−200 ~ 0 ms)各通道信号求标准差,定义基线段内各通道信号标准差异常的通道为坏通道,使用与坏通道之间欧式距离最近的4个通道的信号均值进行坏通道修正。计算单个试次中各个通道的标准差,对所有试次的每个通道进行IQR异常值检测,若一个试次中存在任意一个通道的标准差异常,则认为该试次为坏段[14]。坏通道插值与坏试次剔除后的MEG信号绘制平均诱发响应图,用于观测与分析M100尖峰。在听觉诱发场中,将不同探测器距离下的脑磁信号信噪比(signal-to-noise ratio, SNR)作为主要评价指标,其定义为:

$$SNR = 20lg\frac{\sum_{i\in ch}\left|\overline{M_{signal,i}}\right|}{\sum_{i\in ch}\sqrt{\sigma_{noise,i}}}$$

其中,$\overline{M_{signal,i}}$表示第i个通道信号段内的幅值均值,$\sigma_{noise,i}$表示第i个通道的噪声方差。叠加平均信号的均方根(root mean square, RMS)的最大时刻为M100潜伏期,将M100潜伏期前后10 ms作为响应信号段,刺激出现前100 ms作为噪声段[15]。研究表明特定神经元附近的MEG信号响应比整体信号的响应更有区分性[16],因此选择信号段内RMS最大的3个通道用于SNR指标分析。由于系统在信号触发和音调传递到达被试之间有26 ms的延迟,因此所有潜伏期都进行了26 ms的延迟校正。

最后,使用基于MATLAB的Brainstorm工具箱对M100峰值时刻进溯源分析。将受试者光学扫描得到的面部点云文件以及FreeSurfer分割后的MRI导入Brainstorm。以MRI鼻根点、左耳前、右耳前基准点,与光学扫描得到的面部信息进行配准。依据受试者的MRI,构建5 mm规则的网格源空间。利用重叠球体算法(overlapping spheres)构建受试者的正向模型,最小范数估计(minimum norm estimate)解决线性逆问题,对预处理后的脑磁数据进行溯源,使用目视检查方法[17-18]对各条件下溯源位置进行定性分析。

1.6 统计学方法

统计分析使用IBM SPSS 24.0进行,使用双样本t检验比较男女年龄和头围的差异。在一般项目的比较中,采用重复测量单因素方差分析,$P<0.05$为差异有统计学意

义。以探测器与头皮间距离为被试内因素, 对4组数据进行重复测量单因素方差分析, 邻近距离间各项指标(噪声、信号强度、SNR、潜伏期)的差异用Bonferroni法进行P值校正, $P<0.0083$为差异有统计学意义。

2　结果

2.1　基本人口统计学信息

本研究共招募了40名健康受试者(20名男性, 20名女性), 平均年龄为(27.08±3.96)岁, 其中男性为(27.40±4.97)岁, 女性为(26.75±2.71)岁, 两组年龄差异无统计学意义($t=0.76$, $P=0.45$)。男性头围为(54.62±1.81) cm, 女性头围为(55.8±6.31) cm, 头围差异也无统计学意义($t=-0.81$, $P=0.43$)。

2.2　听觉响应信号统计结果

听觉响应信号的噪声、信号强度、SNR、潜伏期这4项数据, 见表1。通过重复测量单因素方差分析发现探测器与头皮间距离对噪声($F_{3,37}=8.51$, $P<0.001$, $\eta_p^2=0.41$)、信号强度($F_{3,37}=92.62$, $P<0.001$, $\eta_p^2=0.88$)和SNR($F_{3,37}=15.96$, $P<0.001$, $\eta_p^2=0.56$)有影响, 而潜伏期($F_{3,37}=2.53$, $P=0.072$, $\eta_p^2=0.17$)则没有。之后两两比较分析相邻条件间的差异, 噪声随着距离的增加, 呈下降趋势, 相邻两组间均没有差异(图3A); 信号强度同样随着距离的增加而逐渐减弱, 5 mm与10 mm、10 mm与15 mm相邻两组有差异($P<0.0083$, 图3B); SNR在5 mm最高, 5 mm与10 mm两组间有差异($P<0.0083$, 图3C); 潜伏期随着距离的增加, 表现为增长的趋势, 但相邻两组间均没有差异(图3D)。

2.3　脑磁信号响应结果

受试者在4组距离下, 分别以1 kHz纯音频音调作为标准刺激重复200次, 刺激时长约50 ms, 刺激间隔为0.8 ~ 1.1 s随机, 均可诱发出M100(表1), 图4展示了一名受试者的叠加平均诱发响应图。

表 1　探测器与头皮不同距离时的指标

Table 1　Metrics at different distances between the detector and the scalp

Index	Detector-to-scalp distance ($\bar{x}\pm s$)				F	P	η_p^2
	0 mm	5 mm	10 mm	15 mm			
Noise/fT	30.56±9.45	26.80±10.91	25.23±9.57	20.68±8.46	8.51	<0.001	0.41
Signal/fT	302.86±121.69	261.73±80.53	183.45±63.23	143.18±60.24	92.62	<0.001	0.88
Signal-to-noise ratio/dB	19.61±3.66	19.98±3.21	17.30±3.52	16.66±3.93	15.96	<0.001	0.56
Latency/ms	100.63±16.52	108.25±21.88	113.95±35.69	111.48±31.81	2.53	0.072	0.17

η_p^2 ranges from 0 to 1 and is used to represent the effect size in ANOVA, with a larger value indicating a larger difference. n=40.

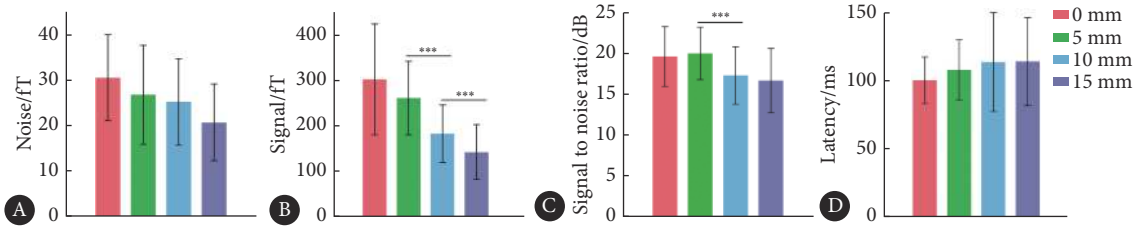

图 3　不同距离下噪声、信号强度、信噪比和潜伏期

Fig 3　The noise, signal strength, signal-to-noise ratio, and latency at different distances

A, Noise gradually weakens with the increase in distance, and no statistically significant difference was found between any neighboring conditions. B, Signal strength gradually weakens with the increase in distance, showing statistically significant differences between 5 and 10 mm and between 10 and 15 mm. C, Signal-to-noise ratio begins to gradually weaken at 10 mm, showing statistically significant differences between 5 and 10 mm. D, Latency is relatively stable at all distances, showing no statistical difference between neighboring conditions. *** $P<0.0083$. n=40.

2.4　脑磁信号溯源结果

本研究对不同距离下采集到听觉脑磁信号进行了溯源定位, 在不同距离下溯源定位结果基本一致, 图5展示了一名受试者溯源定位结果。

3　讨论

OPM是一种新兴的MEG技术, 探测器到头皮距离对信号探测质量的影响尚未得到系统研究, 而这一因素可能直接影响OPM对神经信号的探测能力。本研究的目的在于通过调整OPM探测器到头皮的距离, 分析不同距离下颞叶听觉诱发响应信号的强度、噪声、SNR和潜伏期的变化, 进而证明OPM信号采集的有效性。

首先, 本研究发现, 随着探测器距离增加, 信号强度和噪声呈线性衰减趋势。神经活动产生的生物磁场极其

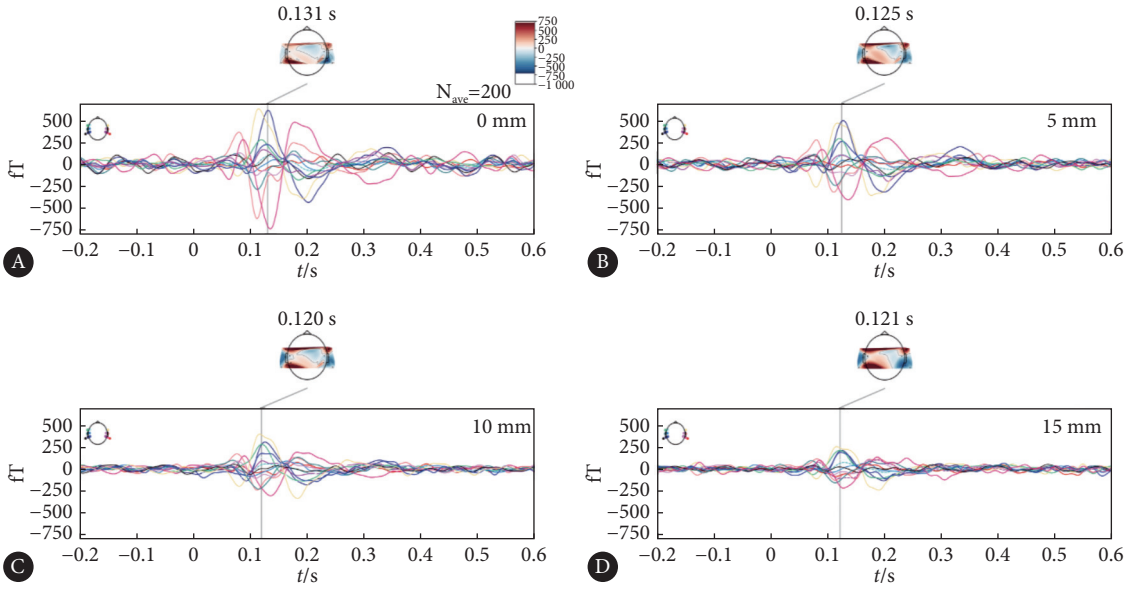

图 4 一名受试者在不同距离下采集到的脑磁信号叠加平均诱发响应图

Fig 4 Evoked responses of electromagnetic brain signals acquired from one subject at different distances

M100 evoked response at 0 mm (A), 5 mm (B), 10 mm (C), and 15 mm (D) detector-to-scalp distance, respectively.

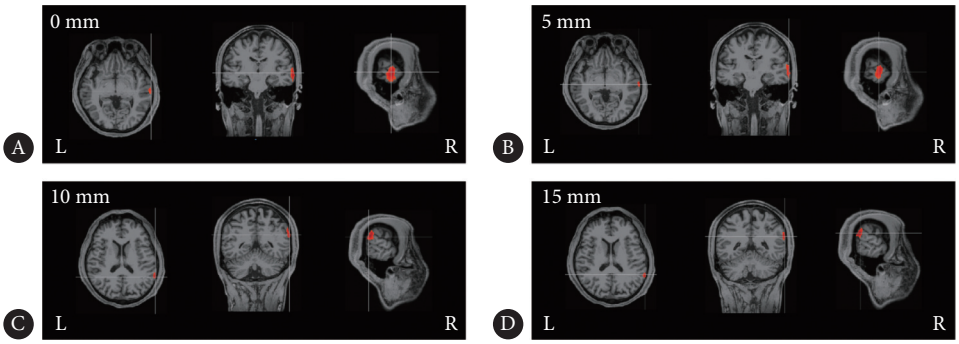

图 5 一名受试者在不同距离下采集到的脑磁信号溯源结果

Fig 5 Source reconstruction of brain magnetic signals acquired at different distances in one subject

Auditory stimulus source reconstruction results at 0 mm (A), 5 mm (B), 10 mm (C), and 15 mm (D) detector-to-scalp distance, respectively.

微弱，强度通常在50 ~ 500 fT范围内[19]，OPM-MEG能够探测到此类信号，并且随着探测器与头皮的距离增加，信号强度通常会逐渐减弱[20]。本研究中，观察到的趋势与以往研究一致。同时，随着距离增大，噪声也相应减少，可能是由于距离增大使得由生理信号引入的噪声减少的缘故。结果表明，在5 mm处SNR最佳。SNR越高，表明系统的抗干扰能力越强[21]。以上结果提示，在临床应用中，探测器与头皮间无需紧贴(0 mm)即可获得良好的检测效果，这一结果有助于优化临床操作的便捷性。

在以往的研究中，通常将探测器与头皮的距离设定为：要么尽量贴近头皮[21-22]，要么固定在某个特定距离，如5 mm[23]、6.5 mm[13]等。然而，在临床的实际使用中，由于被试的头型大小不一、使用者的习惯各异，无法实现探测器与受试者头皮的距离统一，因此需要确定距离对信号质量的影响。本研究结果显示，尽管不同距离下信号幅度有所衰减，SNR也会下降，但即使在15 mm距离下，SNR仍可达(16.66±3.93) dB，高于URBAN等[15]研究中的11.1 dB。这表明即便在相对较远的距离下，OPM探测器也能够保持有效的信号采集，进一步证明了其适应临床需求的潜力。

此外，本研究发现不同距离下M100峰值的潜伏期无显著差异，且与相关文献报道的一致[15, 24-25]，显示了该设备在不同距离下听觉信号响应时间的一致性。对M100峰值溯源分析发现，不同距离下溯源结果基本一致，这为OPM-MEG信号采集的空间一致性提供了进一步证据，证明了其在实际应用中的稳定性。总的来看，本研究结果证明了OPM-MEG采集听觉诱发响应信号的有效性，有望成为评估患者响应能力的有效手段之一。

本研究探讨了不同探测器与头皮间的距离对颞叶听

觉反应信号幅度、噪声、SNR和潜伏期的影响。结果表明, 在5 mm距离处, SNR达到峰值并达到最佳稳定性, 即使在15 mm距离处, SNR仍保持在16 dB以上, 满足临床要求, 证明了OPM-MEG的有效性。但本研究并未提供精确源定位的定量结果, 未来的研究将针对癫痫等明确病变的患者, 验证该技术在病理性脑信号采集中的有效性。此外, 研究团队计划将样本扩大到高海拔人群, 旨在探究长时间高海拔暴露对神经功能区域和信号特征的影响, 这些发现可能支持神经系统疾病的诊断和预防。

*　　*　　*

作者贡献声明　袁媛负责论文构思、正式分析、提供资源和初稿写作, 陈正举负责论文构思、调查研究、研究方法和初稿写作, 孙伟和付诗琴负责研究项目管理, 金琳和孟秋建负责数据审编、正式分析、验证和可视化, 盛经纬和武江芬负责经费获取和研究项目管理, 陈蕾和幸浩洋负责监督指导和审读与编辑写作。所有作者已经同意将文章提交给本刊, 且对将要发表的版本进行最终定稿, 并同意对工作的所有方面负责。

Author Contribution　YUAN Yuan is responsible for conceptualization, formal analysis, resources, and writing--original draft. CHEN Zhengju is responsible for conceptualization, investigation, methodology, and writing--original draft. SUN Wei and FU Shiqin are responsible for project administration. JIN Lin and MENG Qiujian are responsible for data curation, formal analysis, validation, and visualization. SHENG Jingwei and WU Jiangfen are responsible for funding acquisition and project administration. CHEN Lei and XING Haoyang are responsible for supervision and writing--review and editing. All authors consented to the submission of the article to the Journal. All authors approved the final version to be published and agreed to take responsibility for all aspects of the work.

利益冲突　本文作者盛经纬持有北京昆迈医疗科技有限公司股份, 金琳和孟秋建为该公司员工, 但仪器和软件均非该公司免费提供。本文作者陈蕾是本刊编委会青年编委, 该文在编辑评审过程中所有流程严格按照期刊政策进行, 且未经其本人经手处理。除此之外, 所有作者均声明不存在利益冲突。

Declaration of Conflicting Interests　SHENG Jingwei holds shares of Beijing Quanmag Healthcare, and JIN Lin and MENG Qiujian are employees of the company. However, none of the equipment and computer programs used in the study were provided free of charge by the company. CHEN Lei is a member of the Junior Editorial Board of the journal. All processes involved in the editing and reviewing of this article were carried out in strict compliance with the journal's policies and there was no inappropriate personal involvement by the author. Other than this, all authors declare no competing interests.

参　考　文　献

[1] CHEN X M, ZHANG Q, WANG J Y, *et al*. Cognitive and neuroimaging changes in healthy immigrants upon relocation to a high altitude: a panel study. Hum Brain Mapp, 2017, 38(8): 3865-3877. doi: 10.1002/hbm.23635.

[2] MA H L, WANG Y, WU J H, *et al*. Long-term exposure to high altitude affects response inhibition in the conflictmoni toring stage. Sci Rep, 2015, 5: 13701. doi: 10.1038/srep13701.

[3] 何盈, 鲍海华, 王芳芳, 等. 低海拔正常成人移居高海拔地区2 年后脑的适应性变化. 山东医药, 2017, 57(38): 92-94. doi: 10.3969/j.issn.1002-266X.2017.38.030.
HE Y, BAO H H, WANG F F. Adaptive changes in the brain of normal adults at low altitude after a 2-year move to high altitude. Shandong Med J, 2017, 57(38): 92-94. doi: 10.3969/j.issn.1002-266X.2017.38.030.

[4] BARRATT E L, FRANCIS S T, MORRIS P G, *et al*. Mapping the topological organisation of beta oscillations in motor cortex using MEG. Neuro Image, 2018, 181: 831-844. doi: 10.1016/j.neuroimage.2018.06.041.

[5] UHLHAAS P J, LIDDLE P, LINDEN D E J, *et al*. Gross Magnetoencephalography as a tool in psychiatric research: current status and perspective. Biol Psychiatry Cogn Neurosci Neuroimaging, 2017, 2: 235-244. doi: 10.1016/j.bpsc.2017.01.005.

[6] 陈春巧, 张欣, 郭清乾, 等. 基于原子磁力计的穿戴式脑磁图动态测量研究. 波谱学杂志, 2022, 39(3): 337-344. doi: 10.11938/cjmr20222975.
CHEN C Q, ZHANG X, GUO Q Q, *et al*. Moving wearable magnetoencephalography measurement study based on optically-pumped magnetometer. Chin J Magn Reson, 2022, 39(3): 337-344. doi: 10.11938/cjmr20222975.

[7] VRBA J. Magnetoencephalography: the art of finding a needle in a haystack. J Psychophysiol, 2003, 17(4): 237-237. doi: 10.1016/S0921-4534(01)01131-5.

[8] MUKAMEL R, GELBARD H, ARIELI A, *et al*. Coupling between neuronal firing, field potentials, and FMRI in human auditory cortex. Science, 2005, 309(5736): 951-954. doi: 10.1126/science.1110913.

[9] SHAH V K, WAKAI R T. A compact, high performance atomic magnetometer for biomedical applications. Phys Med Biol, 2013, 58: 8153-8161. doi: 10.1088/0031-9155/58/22/8153.

[10] BOTO E, HOLMES N, LEGGETT J, *et al*. Moving magnetoencephalography towards real-world applications with a wearable system. Nature, 2018, 555: 657-661. doi: 10.1038/nature26147.

[11] DANG H B, MALOOF, ROMALIS M V. Ultra-high sensitivity magnetic field and magnetization measurements with an atomic magnetometer. Appl Phys Lett, 2010, 97(15): 151110. doi: 10.1063/1.3491215.

[12] SHENG J, WAN S, SUN Y, *et al*. Magnetoencephalography with a Cs-based high-sensitivity compact atomic magnetometer. Rev Sci Instrum, 2017, 88(9): 094304. doi: 10.1063/1.5001730.

[13] BOTO E, MEYER S S, SHAH V, *et al*. A new generation of magnetoencephalography: room temperature measurements using optically-pumped magnetometers. Neuro Image, 2017, 149: 404-414. doi: 10.1016/j.neuroimage.2017.01.034.

[14] HILL R M, DEVASAGAYAM J, HOLMES N, *et al*. Using OPM-MEG in contrasting magnetic environments. Neuro Image, 2022, 253: 119084. doi: 10.1016/j.neuroimage.2022.119084.

[15] URBAN M, ANNA J, RVDIGER B, *et al*. Transforming and comparing

data between standard SQUID and OPM-MEG systems. PLoS One, 2022, 17(1): e0262669. doi: 10.1371/journal.pone.0262669.

[16] BORNA A, CARTER T R, COLOMBO A P, *et al*. Non-invasive functional-brain-imaging with an OPM-based magnetoencephalography system. PLoS One, 2020, 24;15(1): e0227684. doi: 10.1371/journal.pone.0227684.

[17] YUN S D, SHAH N J. Whole-brain high in-plane resolution fMRI using accelerated EPIK for enhanced characterisation of functional areas at 3T. PLoS One, 2017, 12(9): e0184759. doi: 10.1371/journal.pone.0184759.

[18] ZHAO J, TANG C, NIE J. Functional parcellation of individual cerebral cortex based on functional MRI. Neuroinformatics, 2020, 18(2): 295-306. doi: 10.1007/s12021-019-09445-8.

[19] COHEN D. Magnetoencephalography: detection of the brain's electrical activity with a superconducting magnetometer. Science, 1972, 175(4022): 664-666. doi: 10.1126/science.175.4022.664.

[20] HAMALAINEN M, HARI R, ILMONIEMI R J, *et al*. Magnetoencephalography-theory, instrumentation, and applications to noninvasive studies of the working human brain. Rev Mod Phys, 1993, 65(2): 413. doi: 10.1103/RevModPhys.65.413.

[21] 胡广书. 数字信号处理——理论、算法与实现(第3版). 北京: 清华大学出版社, 2012.

HU G S. Digital signal processing - Theory, algorithms and implementation (3rd Edition). Beijing: Tsinghua University Press, 2012.

[22] ALEM O, HUGHES K J, BUARD I, *et al*. An integrated full-head OPM-MEG system based on 128 zero-field sensors. Front Neurosci, 2023, 17: 1190310. doi: 10.3389/fnins.2023.1190310.

[23] AN K M, SHIM J H, KWON H, *et al*. Detection of the 40 Hz auditory steady-state response with optically pumped magnetometers. Sci Rep, 2022, 12(1): 17993. doi: 10.1038/s41598-022-21870-5.

[24] PAMTEY C, EULITZ C, ELBERT T, *et al*. The auditory evoked sustained field: origin and frequency dependence. Electroencephalogr Clin Neurophysiol, 1994, 90(1): 82-90. doi: 10.1016/0013-4694(94)90115-5.

[25] 王宝山, 苗英章, 朱庆文, 等. 听神经病大脑听觉皮层功能区脑磁图初步观察. 中华耳鼻咽喉头颈外科杂志, 2006, 41(5): 346-350. doi: 10.3760/j.issn:1673-0860.2006.05.008.

WANG B S, MIAO Y Z, ZHU Q W, *et al*. Preliminary study on the functional localization of auditory cortex in auditory pathyology patients using magnetoencepahalography. Chin J Otorhinolaryngol Head Neck Surg, 2006, 41(5): 346-350. doi: 10.3760/j.issn:1673-0860.2006.05.008.

（2024－04－23收稿, 2024－10－11修回）

编辑 吕 熙